Multi-field behavior of Relaxivity in an Iron-rich environment

N. R. Ghugre[1,2], P. Storey[3], C. K. Rigsby[4,5], A. A. Thompson[4,6], C. L. Carqueville[5], T. D. Coates[7], and J. C. Wood[1,2]

[1]Division of Cardiology, Childrens Hospital Los Angeles, Los Angeles, CA, United States, [2]Department of Radiology, Childrens Hospital Los Angeles, Los Angeles, CA, United States, [3]Department of Radiology, New York University School of Medicine, [4]Feinberg School of Medicine, Northwestern University, Chicago, IL, United States, [5]Department of Medical Imaging, Childrens Memorial Hospital, Chicago, IL, United States, [6]Department of Pediatrics, Childrens Memorial Hospital, Chicago, IL, United States, [7]Division of Hematology-Oncology, Childrens Hospital Los Angeles, Los Angeles, CA, United States

Introduction: MRI has gained clinical acceptance as a non-invasive tool to monitor tissue iron stores in patients with iron overload syndromes. Relaxivity parameters R2 (1/T2) and R2* (1/T2*) have been calibrated with clinical accuracy on 1.5T scanners to quantify hepatic iron concentration (HIC) (1, 2). R2* rises linearly with HIC while R2 has a curvilinear relationship. With the increase in migration to 3T scanners, there is need to translate these calibration curves to higher fields. In this regard, tissue biopsy is not a very practical approach. Alternatively, a recent study (3) established the relationship between R2* at 3T and 1.5T over a wide range of HIC; R2* increased two-fold with field strength. However, a similar field-dependent calibration for R2 is currently lacking. Moreover, due to the non-linear nature of the R2-iron relationship, it is unclear whether R2 scales linearly with field strength. Toward this end, we followed a computational approach by generating realistic (iron overloaded) liver geometries and simulating R2 and R2* imaging experiments. Such a model has already been successful in predicting R2-iron and R2*-iron relationships within tolerable limits (4). Here we extend the model to interrogate the relaxivity enhancement brought about by a wide range of field strengths. To validate and compare the predictions of the model, we also performed R2 and R2* imaging at 1.5T and 3T in the livers of patients with transfusional iron burden. A model-based approach will eliminate the need to recalibrate in patients for changes in sequence type, sequence parameters and imaging conditions.

Methods: 80 μm side (cuboidal) 'virtual' liver geometries with 64 hepatocytes were generated for HIC in the range of 0.5-60 mg/g dry tissue weight, as previously described (4). Magnetic susceptibility of impenetrable spherical iron deposits was computed as a 4:1 mixture of hemosiderin and ferritin using literature values. 5000 protons were allowed to perform a random walk (diffusion coefficient = 0.76 μm^2/ms) through the magnetic environment and field induction decays were computed using their phase accruals (R2* measurement). A single echo experiment was also simulated to measure R2 with echo times (TE) logarithmically spaced between 0.1-30 ms. Simulations were performed for field strengths varying between 0.25-7T. The model neglected any contact or exchange mechanisms.

MRI measurements were performed on thalassemia major patients using phased array coil on 1.5T and 3T GE Signa Twinspeed systems. Liver R2* was measured (16 patients) in a single mid-hepatic slice using single-echo gradient echo sequence as described in (3). Liver R2 was measured (6 patients) in 4 slices using a 90°-90° Hahn spin echo sequence with TR=300ms, TE_{min}=3ms (4ms at 3T), TE_{max}=70ms, BW=62.5 kHz, NEX=1 and matrix size=64x64. R2 values were computed in 16 regions of interest (4 per slice) by fitting the mean signal decay to an (exponential+constant) model.

Results: (Let *x* and y represent the horizontal and vertical axes respectively). Fig. 1 shows the relationship between 3T and 1.5T R2*. Both model and patient data demonstrated a two-fold increase in R2* at 3T. Bland-Altman analysis showed that difference in patient and model-predicted R2* values was not statistically significant (standard deviation = 13.8%). Fig. 2 shows 3T vs. 1.5T R2; model-predicted relationship was highly linear with an R^2 of 0.9958. There was no statistical difference between patient and predicted R2 according to Bland-Altman analysis (standard deviation = 7.24%). A regression slope of 1.47 indicated that R2 did not increase linearly with field strength.

Model-predicted (X T vs 1.5T) plots, where X=0.25-7T, demonstrated extremely tight regression lines with minimum R^2 = 0.9905 (for R2) and 0.9967 (for R2*). We refer to the (X T vs 1.5T) regression slope as relaxivity enhancement (RE). Fig. 3 shows the RE computed by simulating a range of field strengths; the relationship is linear for R2* as expected but curvilinear for R2 (linear in log-log scale). The equations are given by, $RE_{R2}(X) = \exp(-0.22 + 0.56*\log(X))$ and $RE_{R2*}(X) = -0.0086 + 0.68*X$. Hence, if R2 and R2* calibration curves are known at 1.5T, they can be translated to other field strengths using, $R2(X) = R2(1.5T) * RE_{R2}(X)$ and $R2*(X) = R2*(1.5T) * RE_{R2*}(X)$.

Discussion: With increasing popularity of 3T scanners, it is important to characterize R2 and R2* behavior in relaxivity-based high-field clinical applications. Using liver as a 'model' tissue, we demonstrate here that a realistic tissue model can be used to translate relaxivity-iron calibration curves to higher field strengths. As we move to higher fields, magnetic perturbers cause the MRI signal to decay very rapidly. R2* being linear with field, is limited by the allowable minimum echo time. Hence, R2* calibration will be restricted to the lower half of the clinically-relevant HIC. On the other hand, the non-linear field dependence of R2 will predict a reasonable upper limit of iron burden with a standard minimum TE. A limitation of the study was that R2 imaging was performed only on 6 patients. However, these formed a wide range of HIC measurements (~3-35 mg/g dry wt.) (2) and were in excellent agreement with the model. Future multi-field comparisons in large patient populations will help reinforce the model validation. On a different note, iron calibration curves have been obtained for CPMG sequences as well (5, 6, 7); these are different compared to spin echo R2 relationships. The model can be used to interrogate complicated CPMG behavior and expose underlying mechanisms of inter-echo spacing and field dependent R2 behavior (5). With that said, the real power of the model lies in predicting iron-mediated R2 and R2* without having to perform tissue biopsies and re-scan patient cohorts for new sequences and clinical sites.

Acknowledgements: GCRC (RR00043-43), NIH (1 R01 HL75592-01A1), Saban Research Institute (CHLA), The Wright Foundation.

References: 1) St Pierre TG, Clark PR, Chua-anusorn W, et al., Blood 2005; 105:855-861.
2) Wood JC, Enriquez C, Ghugre N, et al., Blood 2005; 106:1460-1465.
3) Storey P, et. al., J Magn Reson Imaging. 2007 Mar; 25(3):540-7.
4) Ghugre N, et. al. Proc. Intl. Soc. Mag. Reson. Med 15, 2007; 1780.
5) Bulte JW, et. al., Magn Reson Med. 1997 Apr;37(4):530-6.
6) Ghugre N, Coates TD, Nelson MD, Wood JC, Mag Res Med 2005; 54:1185-1193.
7) Alexopoulou E, et. al., J Magn Reson Imaging. 2006 Feb;23(2):163-70.

Figure 1

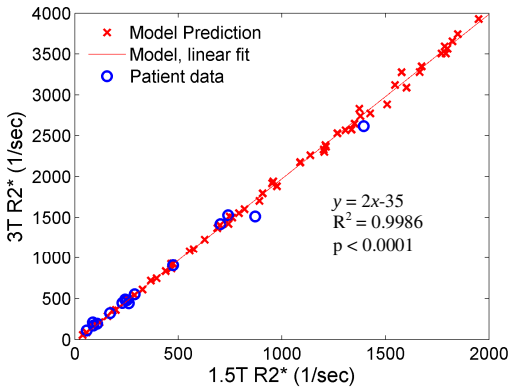

Figure 2

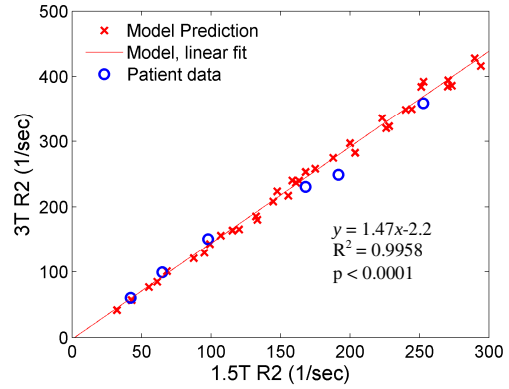

Figure 3